Development of Polyaniline using electrochemical technique for plugging pinholes in Cadmium Sulfide/Cadmium Telluride Solar Cells

ABDUL-MANAF, N. A., ECHENDU, O. K., FAUZI, F., BOWEN, L. and DHARMADASA, I <http://orcid.org/0000-0001-7988-669X>

DEVELOPMENT OF POLYANILINE USING ELECTROCHEMICAL TECHNIQUE FOR PLUGGING PINHOLES IN CADMIUM SULFIDE/CADMIUM TELLURIDE SOLAR CELLS

N.A. Abdul-Manaf[a*], O.K. Echendu[a], L. Bowen[b] and I.M. Dharmadasa[a]

[a]Electronic Materials and Sensors Group, Materials and Engineering Research Institute, Faculty of Arts, Computing, Engineering and Sciences, Sheffield Hallam University, Sheffield S1 1WB, United Kingdom.
[b]Department of Physics, Durham University, South Road, DH1 3LE Durham, United Kingdom.
Email: azlian_manaf@yahoo.co.uk*

Tel: +44(0)114 2256910 Fax: +44(0)114 2256930

Abstract: Polyaniline (PAni) thin films were prepared by an electrochemical polymerization technique on glass/FTO substrates by varying deposition potential, deposition time, pH concentrations and heat treatment conditions. The structural, morphological, optical and electrical properties of electrodeposited PAni films were characterised using XRD, SEM, UV-VIS Spectroscopy, optical profilometer and DC conductivity measurement. Structural analysis shows the formation of highest crystalline emeraldine salt phase of polyaniline at a cathodic potential of 1654 mV. Optical absorption measurements have demonstrated a wide variety of energy bandgap (E_g) varying from ~0.50 to 2.40 eV for polyaniline grown by tuning the pH value during the deposition. The electrical resistivity showed an increase from 0.37×10^6 Ωcm to 3.91×10^6 Ωcm when the pH increased from 2.00 to 6.50. The diode structures of glass/FTO/CdS/CdTe/polyaniline/Au were fabricated incorporating polyaniline as a pinhole plugging layer, and assessed for their photovoltaic activities. The results show the enhancement of all device parameters, especially in open circuit voltage and fill factors. This improvement offers a great potential for enhancing solar cell performance and the lifetime, and the latest results are presented in this paper.

Keywords: polyaniline, electrodeposition, pinhole plugging, CdS/CdTe solar-cell

1. INTRODUCTION

A typical thin film cadmium telluride (CdTe) solar cell consists of glass/FTO/CdS/CdTe/metal contact structure. All the films are deposited using electrochemical deposition (ED) except for the FTO and metal contact. ED has demonstrated numerous advantages due to its simplicity, low-cost and suitability for the production of macro scale devices such as solar panels [1].

During the fabrication process of thin film solar cell devices, pin holes are formed for various reasons [1,2]. Pinholes are small areas with a missing layer of the semiconducting cadmium sulphide (CdS), cadmium telluride (CdTe) or both layers. These pinholes are entropy driven and are formed randomly. The pinholes can arise from incomplete coalescence of the CdTe grains during deposition, or be due to defects in the underlying

surface, and are a continuing concern in thin film polycrystalline devices. If these pinholes are left untreated, they will lead to short-circuit the photovoltaic devices after deposition of a metal contact. In order to prevent this, one good solution has been proposed. This involves filling these pinholes with an organic polymer such as polyaniline (PAni) and leaves a very thin layer on the surface to decouple the metal contact and the CdTe layer.

Semiconductor polymers have been widely studied due to their potential applications in numerous research areas including electronics, energy storage, and medicine [3]. Among such polymers, PAni has been studied extensively and is finding increasing uses in various fields of technology such as in anti-corrosion coatings, gas sensors, actuators and light emitting displays (LEDs) [3-6]. PAni is known as a semiconducting polymer, with high tunable bandgap, high chemical stability, processability with a potential application in various fields. PAni comes in three oxidation states, known as leucoemeraldine base, emeraldine base and pernigraniline base (Fig. 1). An oxidation state which is represented by Y will be Y = 1.0 for fully reduced form (leucoemeraldine base), Y = 0.5 for half oxidized (emeraldine base), and Y = 0 for the fully oxidized form (pernigraniline base) [4,5]. A semiresistive PAni (emeraldine salt) can be obtained by doping emeraldine base with protonic acid. During the doping process, the protonic acid allocate the coordination of protons with amine nitrogen of emeraldine base and consequently lead to a charge delocalization in polymer backbone and improve the DC conductivity [5,6]. The properties of PAni can be tuned by changing the pH and growth potential during the electrodeposition.

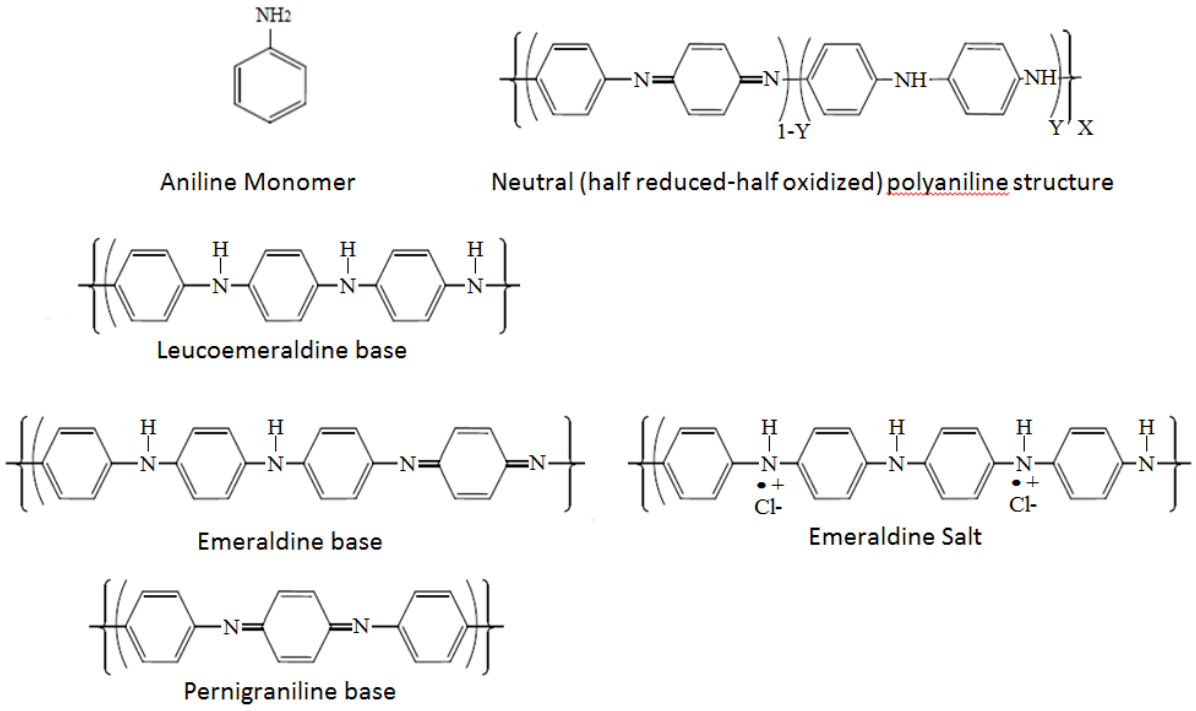

Fig. 1 Aniline monomer, its polymerized forms and possible state of oxidized polyaniline.

This paper reports the experimental approach on deposition of PAni by using electrochemical deposition technique. In view of this, an effort has been made to study the optical and structural properties of PAni deposited at different cathodic potential, growth time, concentrations and pH as well as PAni layers heat treated at different conditions. The effects of PAni as a pin hole plugging layer on CdS/CdTe solar cells are investigated with our preliminary devices and the results are presented and discussed in this paper.

2. MATERIAL AND METHODS

2.1 Materials and substrate preparation

High purity 99.8% aniline and sulphuric acid (H_2SO_4) used in this project were purchased from Sigma Aldrich. The working electrode, fluorine doped tin oxide (FTO) coated glass was cut into 3 x 2 cm^2 pieces. The cleaning process started with rinsing the substrates in soap water, de-ionized water and immersing in acetone solution. These were then rinsed again in de-ionized water and dipped in methanol solution. The substrates were then rinsed in de-ionized water and finally dried up in N_2 gas flow.

2.2 Electrodeposition of Polyaniline thin films

A fresh aniline solution was prepared with 0.1M concentration by dissolving aniline in de-ionized water. The solution was stirred for 15 minutes and initial pH value was measured to be 7.80 ± 0.02. A dilute H_2SO_4 was then added drop by drop until the pH value adjusted to 2.20 ± 0.02. Electrodeposition of PAni was carried out under white light illumination and at room temperature (26 ± 3)^oC using a two electrode system. A carbon electrode was used as the anode (+), while glass/FTO substrate was used as the working electrode, cathode (-). The deposition was performed by applying a cathodic voltage across the glass/FTO cathode with respect to the carbon anode.

During the deposition, aniline monomer polymerized and deposited on negatively charged conductive surface of glass/FTO to form PAni [7]. Before the layer deposition, cyclic voltammogram was obtained in order to estimate the suitable voltage for film deposition. Using the estimated voltage range, PAni layers were grown at different growth voltages (V_g) and the growth conditions were optimized after characterization. The effects of deposition voltage, duration and post-deposition heat treatment at different temperatures on PAni films were studied. The effects of pH variation were also studied by varying pH from 0.50 ± 0.02 to 6.50 ± 0.02.

2.3 Characterization of Polyaniline thin films

The deposited films were then characterized using X-Ray Diffraction (XRD), optical absorption, optical profilometer, scanning electron microscopy (SEM) as well as D.C. conductivity measurements to study their structural, optical, thickness, morphological and electrical properties.

2.4 Voltammogram

Fig. 2 shows the cyclic voltammogram of polyaniline electrolyte during the forward and reverse cycles between 0 to 2000 mV and back to 0 mV. The voltammogram provides information on passage of electric current through the electrolyte and hence the materials deposition details. This has been used to study electropolymerisation of polyaniline and to estimate the suitable voltage range for PAni electrodeposition. The arrows indicate the forward and reverse cycles. The graph shows that electrodeposition of polyaniline starts at ~937 mV while in a reverse sweep, the layer starts to dissolve at ~1100 mV.

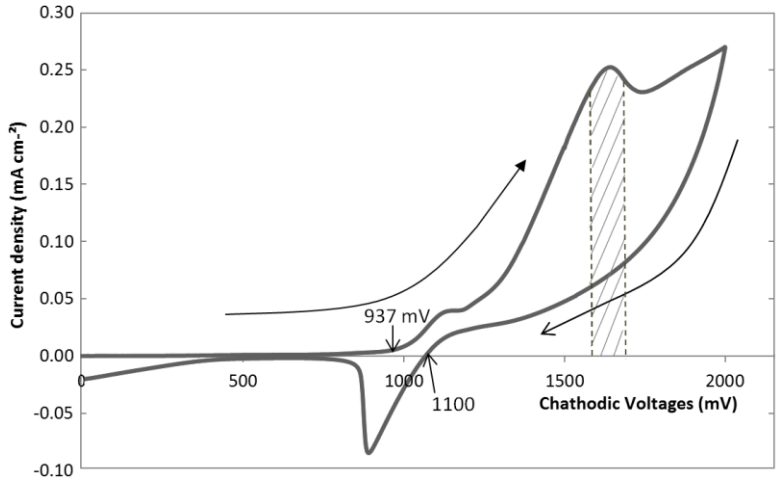

Fig. 2 Cyclic voltamogram for aqueous aniline solution with glass/FTO as the cathode and carbon rod as the anode. The arrows indicate the direction of the cycles.

It was found that there are two small humps which indicate the reduction peak at the cathodic voltage range of ~1100 to ~1200 mV and ~1600 to ~1700 mV, and an exponential onset existing beyond 1800 mV. The electropolymerisation of aniline involves de-electronation and de-protonation of the monomer and the formation of PAni by repeative linking of molecules [5]. The two humps (cathodic peaks) in the voltammogram are due to de-electronation and de-protonation steps which are associated with the partial oxidation of polyaniline to form an emeraldine base. The further rise in the cathodic voltage beyond 1700 mV can be assigned to complete oxidation of aniline to pernigraniline. Indeed, formation of a greenish phase was observed at the cathodic

voltages close to 2000 mV. The detailed study on the cathodic potential around 1650 mV (second peak) was carried out to optimize the V_g for PAni. At higher voltages beyond ~1500 mV, electrolysis of water is also occurring increasing the current through the system and H_2 evolution at the cathode. At the higher voltages, H_2 bubbles could cause delamination of deposited layers.

3. RESULTS AND DISCUSSION

3.1 X-Ray diffraction (XRD) studies

Fig. 3 shows the X-ray diffraction spectra of PAni films grown at different cathodic voltages between 1600 and 1700 mV. By referring to the XRD spectra of FTO substrate (baseline), it is possible to identify four peaks arising from PAni films. The two strongest peaks of PAni are observed at 2θ = 30.7° and 32.1° due to the crystallinity of emeraldine salt phase of PAni [3]. The intensity of these peaks increased as the V_g increased from 1600 to 1654 mV due to benzene-rings settling down on top of another creating a crystalline nature in pernigraniline base. The intensity ratio of emeraldine salt is smaller than that of pernigraniline base. The predominant presence of benzene-ring units in leucoemeraldine base at higher growth potential reduces the intensity of XRD. This indicates that the oxidation level of PANI in the composite increases in the order leucoemeraldine base<emeraldine salt<pernigraniline base [4]. The highest peak of this XRD intensity was obtained at V_g = 1654 mV. There are also two weak peaks appearing at 2θ = 44.0° and 44.9° arising from PAni layer which could be due to the quinoid-ring introduced during the acid-treatment [6]. Therefore in this work, V_g = 1654 mV has been chosen as the optimum potential for electrodeposition of PAni.

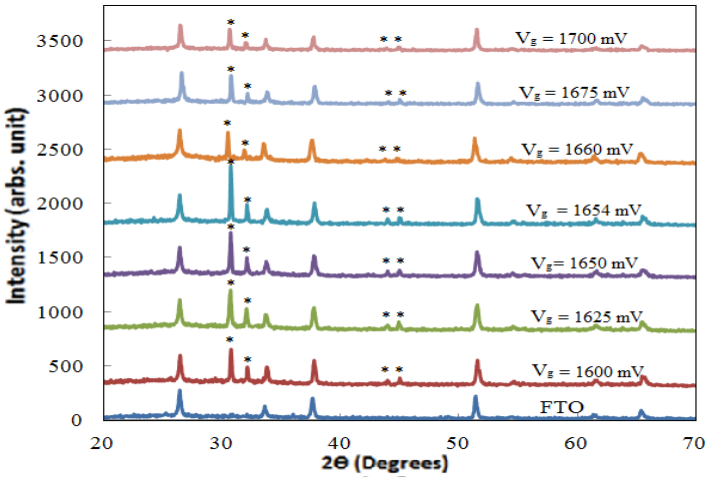

Fig. 3 XRD patterns of polyaniline grown on glass/FTO substrates at different cathodic voltages from 1600 to 1700 mV. Note the best crystallisation at 1654 mV.

Fig. 4 shows the effect of post deposition annealing condition on polyaniline crystalline structure. Three different annealing temperatures (300, 350 and 400^{o}C) have been applied with different duration from two to fifteen minutes. It is observed that the intensity of PAni related peaks increased with annealing in air at 300^{o}C for 5 minutes indicating the optimum heat treatment for best crystallinity, as compared to other conditions. This might be due to the improvement of re-orientation of benzene rings removing any strain created during deposition. Further annealing causes the deterioration of crystallinity reducing XRD peak intensity which might be due to the change in molecular structure arising from deprotonation, oxidation, chain breaking and cross-linking reaction [4,5,6]. Heat treatment of an aromatic hydrocarbon at temperature of 350^{o}C in atmospheric conditions could easily break the bonding in this material forming H_2O and CO_2, reducing the crystalline nature of the PAni layer [6].

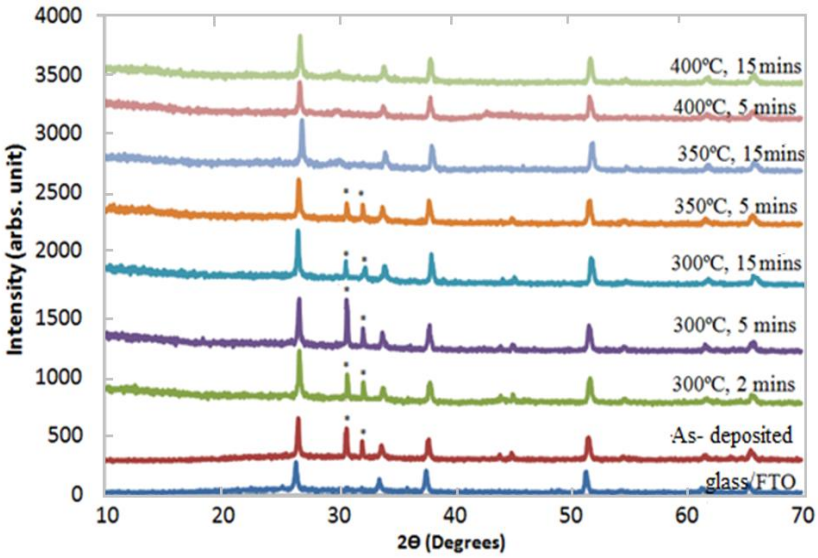

Fig. 4 XRD patterns of PAni layers heat treated at three different temperatures (300, 350 and 400^{o} C) in air for different durations.

3.2 Optical absorption studies

The optical absorption measurements were carried out in order to estimate the energy bandgap of the electrodeposited PAni layers. The value of the bandgap indicates how the material layers perform as absorbers of light. After measuring the optical absorbance (A) as a function of wavelength (λ), the square of absobance (A^2) has been plotted as a function of photon energy to obtain the energy gap (E_g). The bandgaps were estimated by extrapolating the straight line portion of the graph to the photon energy axis.

The effect of heat treatments on bandgap energy has also been studied using optical absorption and the summary of the results are shown in Fig. 5. It was found that the heat treatment increases the bandgap energy from ~0.95 to 2.10 eV with corresponding colour change. As deposited polyaniline layers are emerald green in colour, but after heat treatment at 300^{o}C for 5 minutes in air, the layer became yellow-greenish in colour very similar to the appearance of CdS layer. Fig. 6 shows the appearance of colour of as-deposited and heat treated PAni layers, and compared with the colour of electrodeposited CdS layers. Kang et. al [6] described this observed increase in bandgap upon annealing of PAni sample as arising from the escape of hydrogen molecules which are absorbed and bonded loosely to the PAni layers. At the cathodic voltage of 1654 mV, water splitting is taking place in aqueous solution and therefore hydrogen molecules are evolved at the cathode while the polymerization of aniline is taking place. Therefore, loosely bound hydrogen atoms could be formed in as-deposited PAni layers.

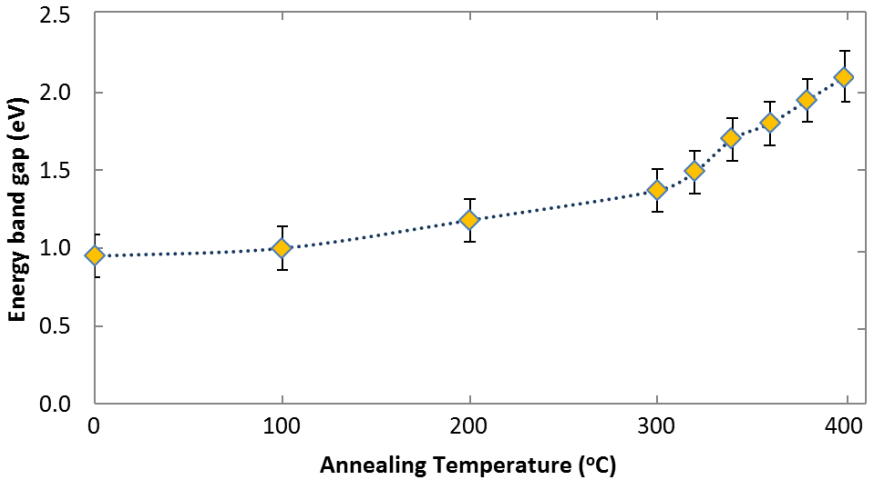

Fig. 5 A typical variation of energy bandgap of PAni layers, as a function of annealing temperature. Duration of annealing at 300^{o}C was kept constant at 5 minutes.

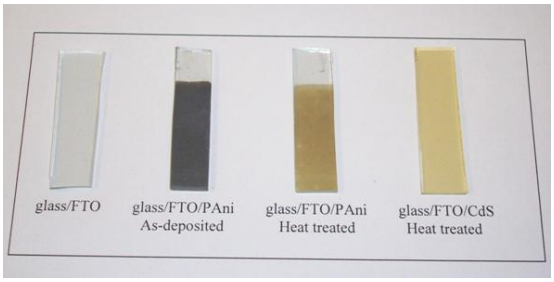

Fig. 6 Images of FTO, as-deposited PAni, heat treated PAni and electrodeposited CdS layers. Note the similar colours of heat treated PAni to CdS layers.

3.3 Scanning electron microscopy (SEM) studies

Scanning electron microscopy was employed to study the surface morphology, grain size and to estimate the thickness of polyaniline layers grown on FTO substrates. Fig. 7(a) presents the surface morphology of polyaniline with a random distribution of grains in the range 99-400 nm. The cross section image (Fig. 7(b)) demonstrates the electrochemically deposited layer of polyaniline for 60 minutes having a wide thickness range from 813 to 1026 nm on the FTO.

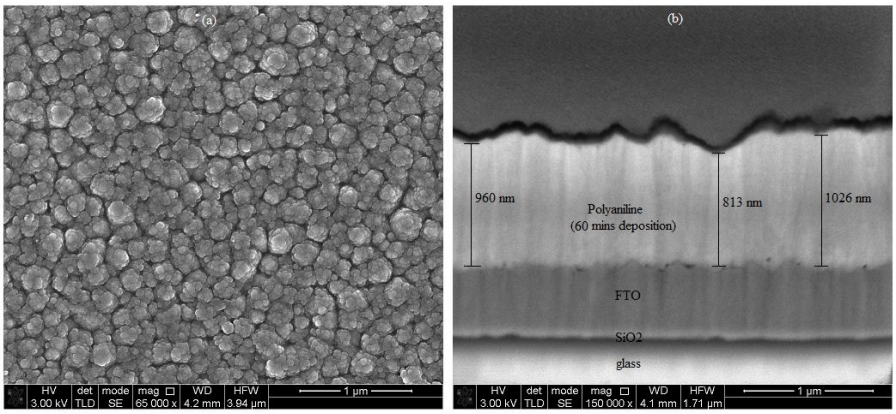

Fig. 7 SEM image of (**a**) a top surface of polyaniline, and (**b**) a cross section of glass/FTO/polyaniline structure. SiO_2 buffer layer used prior to deposition of FTO is also clearly observed.

3.4 Thickness Measurements

The thickness measurements have been carried out in order to estimate the deposition rate for PAni thin films. Five samples were grown at different deposition times varying from 5-60 minutes at a constant deposition voltage of 1654 mV. The thicknesses of these layers were measured with two different methods, using an optical profilometer and the average measurement in SEM cross section images. These two techniques showed similar trends of thickness variation with deposition times, and the results are shown in Fig. 8. The deposition rates estimated from the optical profilometer and the SEM cross section measurements were 14 and 11 nm min^{-1}, respectively. The former value is more accurate due to the difficulties in estimation of thickness from SEM cross sections.

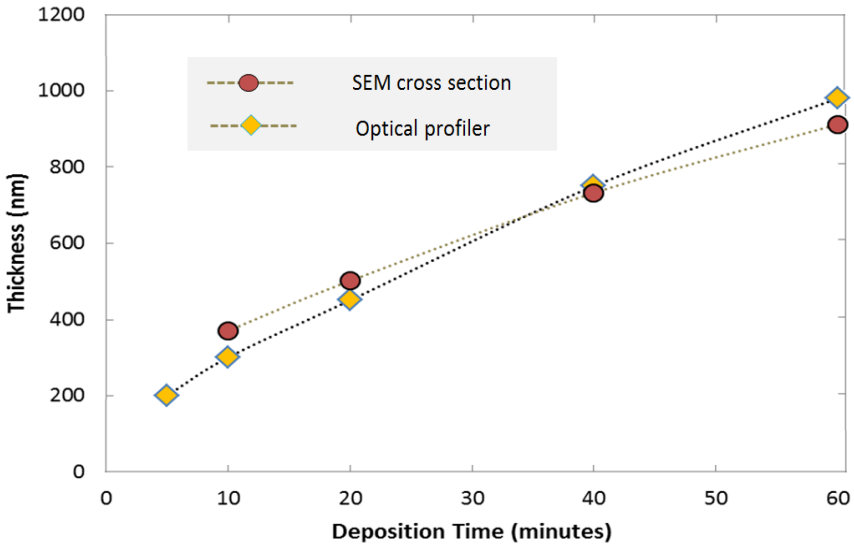

Fig. 8 Comparison of thicknesses of PAni layers as measured using optical profiler and SEM cross section images.

3.5 DC Conductivity Measurements

In order to estimate the electrical conductivity of electrodeposited PAni layers, glass/FTO/PAni/Au structures were fabricated with thick (~950 nm) PAni layers. Au has been used as the metal contact for these studies. I-V measurements were carried out between Au-Au, FTO-Au and Au-FTO in that order while observing their ohmic behaviour. The resistances of the 2 mm diameter Au contacts were estimated and thus the electrical resistivity (ρ) and the electrical conductivity (σ) were estimated with known thicknesses. The measurements were carried out for layers grown at different pH values in order to explore the electrical conductivity variation with the pH value of the electrolyte.

Table 1 summarizes the measurements of average resistance, thickness, resistivity, electrical conductivity and the energy bandgap of PAni layers as a function of the pH values. Figs. 9 and 10 graphically show the variation of E_g and the calculated electrical resistivity as a function of pH values. It demonstrated a wide variety of energy bandgap (E_g) varying from ~0.98 to 2.32 eV while the resistivity of the studied PAni layers vary from 0.37 x 10^6 Ωcm to 3.91 x 10^6 Ωcm with change in pH values from 2.00 to 6.50 during the deposition. Initial oxidation at low pH leads to the formation of radical cations which act as charge carriers. The oxidation of aniline, has to decrease on increasing the pH of the medium due to its deprotonation [8,9]. As a consequence the free charge carriers are getting lower at the higher pH, thus increase the resistivity properties of PAni films [10].

Table 1 The summary of electrical and optical properties of PAni thin films grown at different pH.

pH	Average resistance (Ω)	Resistivity x 10^{6} (Ω cm)	Conductivity x 10^{-6} $(\Omega\ cm)^{-1}$	Energy bandgap (eV)
2.0	20.2	0.37	26.81	0.98
2.5	12.9	0.36	27.12	1.30
3.0	14.9	0.52	19.25	1.56
3.5	12.9	0.81	12.30	1.77
4.0	13.5	0.71	14.16	1.80
4.5	14.6	0.92	10.89	1.83
5.0	15.7	0.82	12.17	1.90
5.5	16.8	2.64	3.78	1.95
6.5	24.9	3.91	2.56	2.32

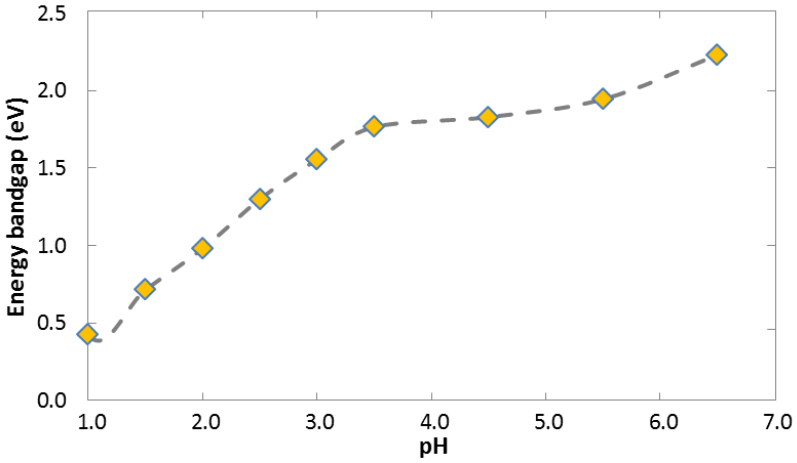

Fig. 9 Energy bandgap of PAni layers grown at different pH value from pH = 1.00 to 6.50. Growth voltage and the duration of growth were kept constant at 1654 mV and 60 min, respectively.

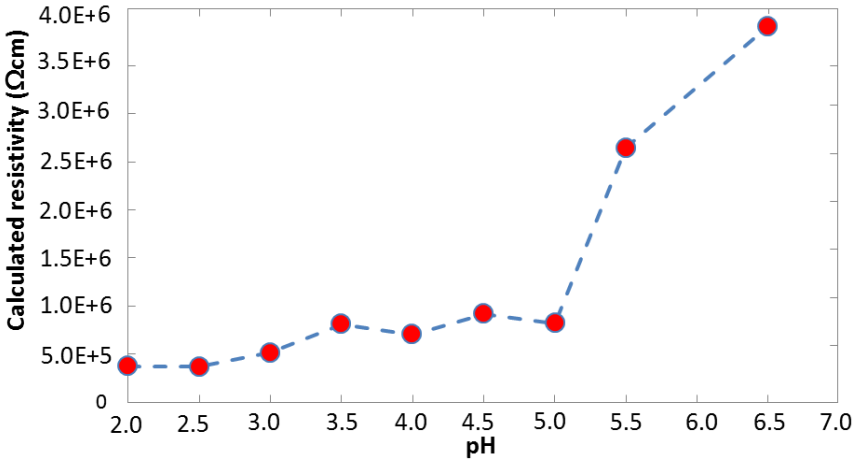

Fig. 10 Resistivity of PAni layers grown as a function of pH value of the electrolyte.

3.6 PAni layers suitable for MIS devices.

Above sections described the growth and characterization of PAni layers at growth voltage of ~1654 mV. That is within the second hump observed in the voltammogram (Fig. 2). However, the films produced by the lowest time period of 10 min is ~300 nm (Fig.8), are not suitable for fabricating MIS structures. Therefore, with the knowledge acquired by this work, it is necessary to establish ultra-thin PAni layers to use in hybrid devices. Those layers should be in the range of few tens of nm, and therefore this section describes the growth of PAni ~1000 mV, within the first hump observed in the voltammogram.

Three samples were grown at voltages between 1100 to 1200 close to the first hump in the voltammogram. These samples were grown with three different growth periods in order to pass approximately equal amount of electronic charges at different growth potentials. By looking at the XRD results, only the sample with V_g = 1150 mV exhibited the appearance of peaks of emeraldine salt phase of PAni at $2\theta = 30.7^o$ and 32.1^o while the others remain amorphous. The thickness have been estimated by optical profilometer in a range of 200 - 350 nm whilst the deposition rate has been calculated and shown in Table 2. The resistivity of all films seems identical with the PAni grown at 1654 mV with pH 5.5 in previous study. The estimated deposition rates are useful in selecty, required thickness of PAni for fabricating MIS devices. for example, 22.2 nm PAni layers can be grown on devices within 10 minutes at V_g 1150 mV.

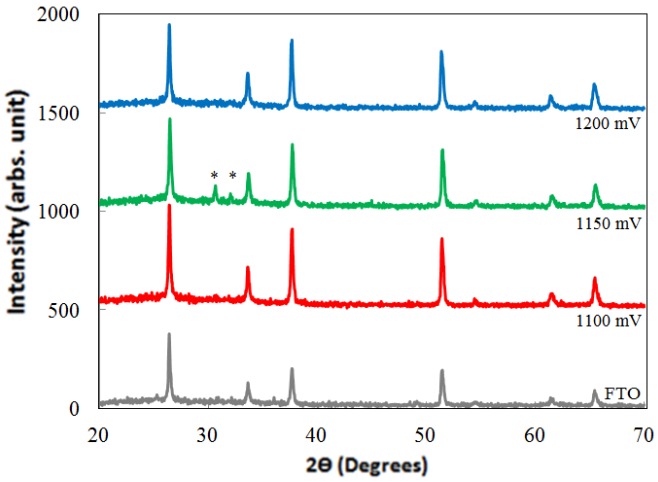

Fig. 11 XRD patterns and optical absorption of polyaniline film grown at three different cathodic voltages: 1100, 1150 and 1200 mV.

Table 2 The deposition time, thickness, deposition rate and resistivity of polyaniline films grown at cathodic potentials of 1100, 1150 and 1200 mV.

Growing Voltage, V_g (mV)	Deposition time (minutes)	Thickness (nm)	Deposition rate (nm min^{-1})	Resistivity x 10^5 (Ω cm)
1100	120	350	1.87	26.6
1150	90	200	2.22	33.7
1200	60	200	3.15	20.8

3.7 Inorganic/Organic hybrid devices

The CdTe based thin film solar cell device structure consists of glass/FTO/CdS/CdTe/back electrical contact. The substrates used in this work are FTO coated glasses. CdS with an energy bandgap of 2.42 eV acts as the window material and CdTe with an energy bandgap of 1.45 eV serves as the absorber material. Both these layers are deposited by electroplating in this work and the thickness of CdS layer is ~100 nm and that of CdTe layer is ~1.8 µm. As reported in ref [11], electroplated CdS and CdTe showed nano- and micro-rods nature. Although these rod-type structures have huge advantages in enhancing solar cell parameters, they also create a disadvantage by producing leakage paths in between these rod-type structures. In this work PAni layers were developed in order to fill these gaps (pin-holes) to avoid short circuiting of solar cell devices and form metal/insulator/semiconductor (MIS) type electrical contact at the back contact. Two types of devices were fabricated with structures of glass/FTO/CdS/CdTe/Au and glass/FTO/CdS/CdTe/PAni/Au to investigate the

effect of PAni in solar cells. Schematic diagram of glass/FTO/CdS/CdTe/PAni/Au is shown in Fig. 12. These devices were then measured using a fully automated I-V system under AM1.5 condition with light intensity of ~100 mW cm^{-2}.

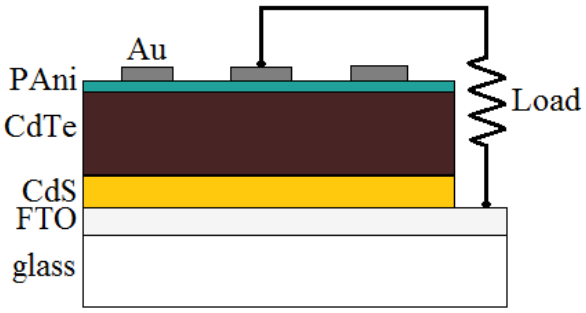

Fig. 12 Schematic diagram of solar cell device with PAni layer incorporated as a pinhole plugging layer (not to scale).

Fig. 13 shows the current-voltage (I-V) characteristics of the glass/FTO/CdS/CdTe/Au and the glass/FTO/CdS/CdTe/PAni/Au solar cell devices under AM 1.5 illumination condition. The result of using PAni as the pinhole plugging layer demonstrated an improvement of all three device parameters as summarized in Table 3. The main improvement came from the fill factor (FF) (22.3%) and the V_{oc} (6.6%). From the I-V curves it is evident that the shunt resistance has increased due to pinhole plugging, and hence the largest improvement was appearing in the FF. The V_{oc} improvement is due to the MIS type electrical contact and the J_{sc} also increase due to reduced leakage.

In the devices with n-type CdTe layers, there exist two PV active junctions; n-n heterojunction at the n-CdS/n-CdTe and a large Schottky diode at n-CdTe/Au contact [11,12, 13,14]. Deposition of ultra-thin insulating PAni creates an MIS type structure at the back contact and therefore it can increase the potential barrier height enhancing the $V_{oc.}$ Ideally, PAni should have insulating properties to completely plug the pin holes and leave a thin film on CdTe. This layer plugs all other conducting paths in the device and contribute to the increase of the shunt resistance (leakage resistance) and thus improving the shape of the I-V curve and hence FF of the device [8]. The efficiency of n-CdS/n-CdTe solar cell improves from 4.9% to 6.5% with insertion of PAni, thus show a clear positive effect of PAni layer in this work. However achieving successful pinhole plugging and effective MIS structures simultaneously could be challenging, but the use of semi-insulating layers solves this issue to a certain level [15]. The resistivity of PAni at ~10^6 Ωcm lies in the semi-insulating region and therefore could work well in device structures. In addition to enhancing all these device parameters, MIS type devices have an

added advantage. The de-coupling of the electrical contact (Au) from the absorber material (CdTe) reduces all interface interaction and hence improves the lifetime of the solar cells.

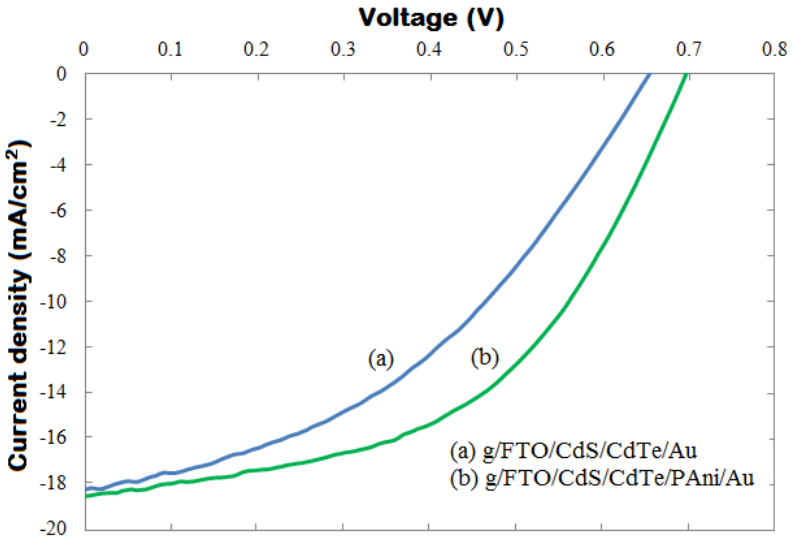

Fig. 13 Current density-voltage characteristics under AM 1.5 condition for solar cells (a) without PAni and (b) with PAni layer of thickness 2.2 nm.

Table 3 Summary of solar cell parameters for the solar cell structures without and with PAni layer.

Device parameters	glass/FTO/CdS/CdTe/Au	glass/FTO/CdS/CdTe/PAni/Au	Percentage improvement
V_{oc} (V)	0.651	0.694	6.6%
J_{sc} (mA cm^{-2})	18.3	18.6	1.71%
FF	0.41	0.50	22.3%
Efficiency (%)	4.9	6.5	32.5%

4. CONCLUSION

The electrochemical synthesis of PAni thin films using acidic and aqueous solution has been successfully established. The PAni layers polymerize well on glass/FTO substrates at cathodic growth voltages of 1654 mV with respect to carbon anode showing the best crystallinity. Post deposition heat treatment at 300^{o}C for 5 min in air improves the crystalline nature of PAni, and beyond this condition, the material loses its crystalline properties. There is a noticeable colour change of the PAni layers on annealing; the dark colour of as-deposited layers (E_g = 0.90 - 1.30 eV) become yellow colour showing bandgap of (E_g~2.20 eV) and appearance close to those of electrodeposited CdS. Preliminary studies of use of PAni as a pinhole plugging layer in n-CdS/n-CdTe solar cell shows improvement in all three device parameters with highest improvement in the FF. This presents a

potential route for the development of low-cost, high efficiency and long lifetime inorganic/organic hybrid thin film solar cells.

ACKNOWLEDGEMENT

The authors would like to thank the Pilkington for providing glass/FTO for this research. The main author also would like to acknowledge the Ministry of Higher Education, Malaysia and National Defence University of Malaysia for financial support.

REFERENCES

[1] M.M. Tessema, M. Giolando, Solar Energy Materials & Solar Cells 107, 9 (2012).
[2] S. K. Das, G. C. Morris, Journal of Applied Physics 72, 4940-4945 (1992).
[3] T. Wang and Y.J. Tan, Corrosion Science 48, 2274 (2006).
[4] Y. Seung-Beom,Y. Eun-Hyea K. Kwang-Bum, Journal of Power Sources 196 (24), 10791 (2011).
[5] J.E. Albuquerqu, L.H.C. Mattoso, D.T. Balogh, R.M. Faria, J. G. Masters, A.G. MacDiarmid, Synthetic Metals 113, 19 (2000).
[6] E.T. Kang, K.G. Neoh, K.L. Tan, Progress in Polymer Science 23, 277 (1998).
[7] B. Basol, Plugged pinhole thin film and method of making same, European patent, EP 0060487A1, Filing date 08.03.1982.
[8] T. A. Skotheim, J. Reynolds, Handbook of Conducting Polymers, 3rd edn (Springer, Marcel Dekker, 2007), pp. 48-54.
[9] G.G Wallace, G. M. Spinks, L.A.P. Kane-Maguire, P. R. Teasdale, Conductive electroactive polymers: intelligent material systems, 3rd edn (CRC Press, 2008) pp. 122-123.
[10] R.K. Pandey, S.N. Sahu and S. Chandra, Handbook of Semiconductor Electrodeposition, (Marcel Dekker: New York, 1996) p. 65.
[11] D. G. Diso, Research and development of CdTe based thin film PV solar cells (Doctoral dissertation), Sheffield Hallam University (2011), http://www.shura.shu.ac.uk/4941/1/Dahiru_Garba_Diso.pdf
[12] I.M. Dharmadasa, I.P. Samantilleke, N.B. Chaure and J. Young, Semiconductor Science and Technology, **17** (12), 1238 (2002).
[13] I.M. Dharmadasa, Advance in Thin Film Solar Cells, (Pan Stanford, 2013), p. 81.
[14] O.K. Echendu , F. Fauzi, A.R. Weerasinghe, I.M. Dharmadasa, Thin Solid Films 556, 529-534 (2014).
[15] N. Romeo, A. Bosio, R. Tedeschi, V. Canevari, Thin Solid Films 361/362, 327 (2000).